

## LUMINACTIVE POLYMETALLIC COMPLEXES

D. Brent MacQueen and John D. Petersen\*

Department of Chemistry, Clemson University, Clemson, South Carolina  
29634-1905 (U.S.A.)

### Summary

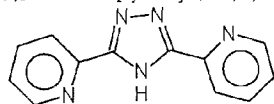
Luminactive (luminescent and photoactive) mono and bimetallic complexes involving the ligand 3,5-bis(2'-pyridyl)-1,2,4-triazole (Hbpt) and its deprotonated form have been studied. In the case of the mono-metallic complexes,  $[\text{RhH}_2(\text{PPh}_3)_2\text{H}_n\text{bpt}](\text{PF}_6)_n$  ( $n = 0$  and  $1$ ), both display luminescence and undergo loss of  $\text{H}_2$  at room temperature in ethanol. The bimetallic complex,  $(\text{bpy})_2\text{Ru}(\text{bpt})\text{RhH}_2(\text{PPh}_3)_2^{2+}$ , undergoes photochemistry from a rhodium-based, ligand-field (LF) excited state and emission from a ruthenium-based metal-to-ligand charge-transfer (MLCT) excited state. These results will be compared to previous studies with other bridging ligands and discussed in terms of intramolecular energy transfer processes.

### INTRODUCTION

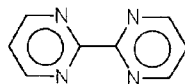
In a previous publication<sup>(1)</sup> we described a multimetallic system of the type  $[(\text{bpy})_2\text{RuLRhH}_2(\text{PPh}_3)_2]^{3+}$  where  $L = 2,2'$  bipyrimidine (bpm), 2,3-bis(2'-pyridyl)pyrazine (dpp), and 2,3 bis(2'-pyridyl)quinoxaline (dpq) and  $\text{bpy} = 2,2'$ -bipyridine in which the compounds are luminactive<sup>(2)</sup> (i.e., both luminescence and photochemistry are observed). Our interpretation was that luminescence occurred from a metal-to-ligand charge-transfer (MLCT) state involving the  $\pi^*$  orbital associated with the bridging ligand. The state responsible for the observed photochemistry was probably a rhodium-based, ligand-field (LF) excited state, populated either directly or *via* energy transfer from a MLCT transition. However, energy transfer *via* population of a ruthenium-based MLCT state involving the LUMO on bpy or the NLUMO on bridging ligand,  $L$ , could not be ruled out.

In attempting to determine if photochemistry occurs *via* energy transfer from a ruthenium-based or rhodium-based MLCT transition or *via* direct population of a rhodium-based LF state, a multimetal complex with

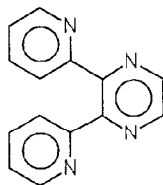
a higher energy  $\pi^*$  LUMO on L was prepared. The bridging ligand chosen was 3,5-bis(2'-pyridyl)-1,2,4-triazole (Hbpt) as Haasnoot *et al.* (3,4) have



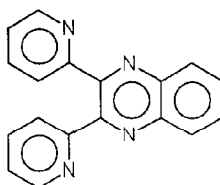
Hbpt



bpm



dpp



dpq

shown that in complexes of the type  $\text{Ru}(\text{bpy})_2\text{bpt}^+$  and  $[\text{Ru}(\text{bpy})_2]_2\text{bpt}^{3+}$  the lowest energy MLCT transition is  $\text{Ru} \rightarrow \text{bpy}$  in nature. Also,<sup>(3)</sup> the bridging ligand  $\text{bpt}^-$  has been shown to facilitate communication between metal sites in the mixed-valence complex,  $[(\text{bpy})_2\text{Ru}^{\text{III}}(\text{bpt})\text{Ru}^{\text{II}}(\text{bpy})_2]^{4+}$ . Thus, the complexes  $[(\text{bpy})_2\text{Ru}(\text{bpt})\text{RhH}_2(\text{PPh}_3)_2]^{2+}$  and  $\text{RhH}_2(\text{PPh}_3)_2\text{bpt}$  were prepared in order to determine the nature of the photoactive state and if any energy transfer processes are occurring.

#### EXPERIMENTAL

All solvents used were reagent grade. The ligand Hbpt<sup>(5)</sup> and the complexes  $[\text{Ru}(\text{bpy})_2\text{bpt}]\text{PF}_6$  (3),  $\{[(\text{bpy})_2\text{Ru}]_2\text{bpt}\}(\text{PF}_6)_3$  (3) and  $[\text{MH}_2(\text{PPh}_3)_2(\text{acetone})_2]\text{PF}_6$  (6) (M = Ir and Rh) were prepared according to literature methods.

The monometallic complex  $\text{RhH}_2(\text{PPh}_3)_2\text{bpt}$  was prepared by the equal molar addition of Hbpt to an acetone solution of  $[\text{RhH}_2(\text{PPh}_3)_2(\text{acetone})_2]\text{PF}_6$ . The volume was reduced and 100% ethanol was added to induce the precipitation of the white solid. The white precipitate was washed with ethanol then ether and dried under vacuum. The infrared spectrum confirmed the compound obtained was  $\text{RhH}_2(\text{PPh}_3)_2\text{bpt}$  and not  $[\text{RhH}_2(\text{PPh}_3)_2\text{Hbpt}](\text{PF}_6)$  as no  $\text{PF}_6$  band was observed at  $840\text{ cm}^{-1}$ .

The heteronuclear bimetallic complexes  $\{[(\text{bpy})_2\text{Ru}]\text{bptM}(\text{PPh}_3)_2\text{H}_2\}(\text{PF}_6)_2$  (M = Ir and Rh) were both prepared by reacting  $[\text{Ru}(\text{bpy})_2\text{bpt}]\text{PF}_6$  with a slight excess of  $[\text{MH}_2(\text{PPh}_3)_2(\text{acetone})_2]\text{PF}_6$  in acetone. In a typical reaction,  $1.2 \times 10^{-4}$  mols of  $[\text{MH}_2(\text{PPh}_3)_2(\text{acetone})_2]\text{PF}_6$  were dissolved in ~10 mL of acetone and  $1.1 \times 10^{-4}$  mols of  $[\text{Ru}(\text{bpy})_2\text{bpt}]\text{PF}_6$  were added to

this solution. The volume was reduced to ~2 mL and 5 mL of 100% ethanol was added. The red precipitate which formed was collected and washed with ethanol to remove the excess  $[\text{MH}_2(\text{PPh}_3)_2(\text{acetone})_2]\text{PF}_6$ , and then with ether to dry the material.

The preparation of monometallic and bimetallic complexes containing bpm, dpp, or dpq have been reported previously.<sup>(1)</sup>

The instrumentation, procedures and measurements utilizing cyclic voltammetry, emission spectroscopy, lifetime measurements, and continuous wave photochemical studies have been reported previously.<sup>(1)</sup>

## RESULTS

The absorption and emission data obtained for the  $\text{bpt}^-$  complexes studied as well as previously reported data for  $\text{bpt}^-$  complexes are given in Table I. The absorption maxima for the rhodium monometallic complexes  $[\text{Rh H}_2(\text{PPh}_3)_2(\text{H}_n\text{bpt})](\text{PF}_6)_n$  ( $n = 0$  and  $1$ ) are similar with maxima at 305 for  $n = 0$  and 293 for  $n = 1$ . These values are similar to the  $\pi-\pi^*$  transitions observed in the deprotonated (318 nm) and neutral (282 nm) bipyridyl triazine ligands.

TABLE I.

Absorption and Emission of Metal Complexes of  $\text{bpt}^-$  and  $\text{Hbpt}$

|                                                                                 | Absorption <sup>a</sup>                         | Emission <sup>a</sup> |                       |                             |
|---------------------------------------------------------------------------------|-------------------------------------------------|-----------------------|-----------------------|-----------------------------|
|                                                                                 | $\lambda_{\text{max}}(\epsilon \times 10^{-4})$ | $\lambda_{\text{em}}$ | $\lambda_{\text{ex}}$ | $\Phi_{\text{em}}$          |
| $[\text{Rh}(\text{PPh}_3)_2\text{H}_2\text{bpt}]$                               | 305 (2.61)                                      | 476                   | 301                   |                             |
| $[\text{Rh}(\text{PPh}_3)_2\text{H}_2(\text{Hbpt})]^+$                          | 293 (3.02)                                      | 432                   | 337                   |                             |
| $[\text{Ru}(\text{bpy})_2\text{bpt}]^+$                                         | 475 <sup>b</sup> (1.13) <sup>b</sup>            | 660                   | 468                   | $7.9 \pm 7 \times 10^{-3}$  |
|                                                                                 |                                                 | 650 <sup>b</sup>      |                       |                             |
| $([\text{Ru}(\text{bpy})_2]_2\text{bpt})^{3+}$                                  | 452 <sup>b</sup> (2.26) <sup>b</sup>            | 628                   | 466                   | $4.6 \pm .5 \times 10^{-3}$ |
|                                                                                 |                                                 | 625 <sup>b</sup>      |                       |                             |
| $[(\text{bpy})_2\text{Ru}(\text{bpt})\text{Rh}(\text{PPh}_3)_2\text{H}_2]^{2+}$ | 459 (1.17)                                      | 630                   | 468                   | $2.0 \pm .1 \times 10^{-2}$ |
|                                                                                 | 430 (1.18)                                      |                       |                       |                             |
|                                                                                 | 289 (8.15)                                      |                       |                       |                             |
| $[(\text{bpy})_2\text{Ru}(\text{bpt})\text{Ir}(\text{PPh}_3)_2\text{H}_2]^{2+}$ | 465 (1.12)                                      | 624                   | 463                   | $1.4 \pm .1 \times 10^{-2}$ |
|                                                                                 | 434 (1.12)                                      |                       |                       |                             |
|                                                                                 | 293 (8.15)                                      |                       |                       |                             |
| Hbpt                                                                            | 282                                             | 427                   | 309                   |                             |
| $\text{bpt}^-$                                                                  | 318                                             | 477                   | 315                   |                             |

<sup>a</sup> In ethanol at 25°C, wavelengths in nm,  $\epsilon$  values in  $\text{M}^{-1} \text{cm}^{-1}$

<sup>b</sup> Reference 3.

The absorption spectra of the two heteronuclear bimetallic complexes  $[(bpy)_2Ru(bpt)MH_2(PPh_3)_2](PF_6)_2$  ( $M = Ir$  and  $Rh$ ) are similar to each other with a low energy maximum of 465 nm for the iridium complex and 459 nm for the rhodium complex. The low energy maximum in the parent ruthenium complex,  $[Ru(bpy)_2bpt]PF_6$ , is at 475 nm thus addition of the second metal center to form the heteronuclear bimetallic complex causes the lowest energy absorption maximum to shift to higher energy. The same shift to higher energy has been reported in the homonuclear bimetallic complex  $\{[Ru(bpy)_2]_2bpt\}(PF_6)_3$  which exhibits a low energy absorption maximum at 452 nm.<sup>(3)</sup>

The absorption spectra of the heteronuclear bimetallic complexes also exhibit two more maxima, one in the visible region and one in the ultraviolet region of the spectrum. In the case of the rhodium bimetallic complex the maxima are at 430 nm and 289 nm while in the iridium complex the maxima are at 434 nm and 293 nm. Similar maxima at 430 nm and 294 nm are observed in the parent ruthenium species,  $[Ru(bpy)_2bpt]PF_6$ .

Based on previous studies of ruthenium(II) polypyridyl mono- and bimetallic complexes,<sup>(3,4,7-11)</sup> the overlapping bands in the heteronuclear bimetallic complexes observed in the 430 nm to 470 nm region are assigned as overlapping MLCT transitions. The ligand involved in the lowest-energy band appears to be associated with the bpy ligand and not the bpt<sup>-</sup> bridging ligand, (see Discussion).

The absorption maxima observed in the 289 nm to 293 nm region of the absorption spectra in the heteronuclear bimetallic complexes are assigned as intraligand  $\pi \rightarrow \pi^*$  transitions. Assignment of these transitions to a specific ligand, bpy or bpt<sup>-</sup>, cannot be made at this time but it is probable that the observed band is the result of overlapping  $\pi \rightarrow \pi^*$  transitions associated with both the bpy and bpt<sup>-</sup> ligands.

The molar absorptivities of the low energy band for the heteronuclear bimetallic complexes,  $[(bpy)_2Ru(bpt)MH_2(PPh_3)_2](PF_6)_3$  ( $M = Ir$  and  $Rh$ ) are very similar to the values reported in the low energy band of the parent ruthenium species,  $[Ru(bpy)_2bpt]PF_6$ . The reported molar absorptivity of the low energy band in the homonuclear bimetallic complex,  $\{[Ru(bpy)_2]_2bpt\}(PF_6)_3$ , is twice that of the monometallic parent complex.<sup>(3)</sup>

The electrically neutral monometallic complex,  $[RhH_2(PPh_3)_2bpt]$ , luminesces in ethanol at 476 nm ( $\lambda_{ex} = 301$  nm). Addition of  $HPF_6$  to the ethanolic solution shifts the emission maximum to 437 nm and the excitation maximum to 337 nm. An emission spectra is observed in both

the neutral and deprotonated form of the free ligand with maxima at 427nm and 477 nm, respectively.

Both of the heteronuclear complexes  $[(bpy)_2Ru(bpt)MH_2(PPh_3)_2](PF_6)_2$  ( $M = Ir$  and  $Rh$ ) luminesce at room temperature. The emission spectrum of the iridium complex displays a maximum at 624 nm ( $\lambda_{ex} = 463nm$ ) while the emission spectra of the rhodium complex exhibits a maximum at 630 nm ( $\lambda_{ex} = 468nm$ ). These values are very similar to the emission maximum of 625 nm ( $\lambda_{ex} = 466nm$ ) reported for the homonuclear bimetallic complex,  $[(Ru(bpy)_2)_2bpt](PF_6)_3$ .<sup>(3)</sup> The emission maxima for the bimetallic complexes are all higher in energy than the maximum of 660nm ( $\lambda_{ex} = 468nm$ ) reported for the emission spectra of the monometallic complex,  $[Ru(bpy)_2bpt](PF_6)$ .<sup>(3)</sup>

Perhaps the most interesting data from the luminescence study is the value obtained for the quantum yields of emission ( $\Phi_{em}$ ). The ruthenium mono-metallic parent complex,  $Ru(bpy)_2bpt^+$ , has a value of  $\Phi_{em} = 7.9 \times 10^{-3}$  while the homonuclear bimetallic complex has a value of  $\Phi_{em} = 4.6 \times 10^{-3}$ . This type of behavior, decreasing  $\Phi_{em}$  with increase in the number of metal centers, is typical of transition metal systems.<sup>(9-12)</sup> However, in the heteronuclear bimetallic complexes,  $[(bpy)_2Ru(bpt)MH_2(PPh_3)_2]^{2+}$  ( $M = Ir$  and  $Rh$ ), the values obtained for  $\Phi_{em}$  are larger than the value for the ruthenium monometallic complex. The value of  $\Phi_{em} = 1.4 \times 10^{-2}$  was obtained for the iridium complex while a value of  $\Phi_{em} = 2.0 \times 10^{-2}$  was obtained for the rhodium complex.

The cyclic voltammetric data for the complexes studied as well as previously reported data are given in Table II for the  $bpt^-$  species. The literature  $E_{1/2}$  values for the  $Ru^{III/II}$  redox couple (0.87 V) in  $[Ru(bpy)_2bpt](PF_6)$  and the  $Ru^{III/II}$  redox couples (1.08V and 1.40V) in  $[(Ru(bpy)_2)_2bpt](PF_6)_3$  agree with the values obtained in this laboratory. We observed two ligand based redox couples in the monometallic ruthenium complex while the reductive electrochemistry for the homonuclear bimetallic complexes is not well behaved. In the monometallic complex  $[Ru(bpy)_2bpt]PF_6$ , two, one-electron reversible redox couples are observed at  $E^1_{1/2} = -1.47V$  and  $E^2_{1/2} = -1.73V$ . In the homonuclear bimetallic complex,  $[(Ru(bpy)_2)_2bpt](PF_6)_3$ , waves which appear to be two, overlapping one-electron redox couples centered at  $\sim -1.39V$  are observed. Scanning beyond  $-1.6V$  leads to the appearance of adsorption and desorption waves. The two ligand-based redox couples observed in the monometallic ruthenium complex are assigned as  $bpy$  based reductions while the complex voltammetry observed in the

TABLE II.

Electrochemical Data for Metal Complexes of bpt.<sup>a</sup>

|                                                                               | $E_{1/2}\text{Ru}^{\text{III/II}}$     | $E_{\text{a}}^{\text{ox}}(\text{Rh, Ir})$ | $E_{1/2}\text{bpy}^{0/-}$ |
|-------------------------------------------------------------------------------|----------------------------------------|-------------------------------------------|---------------------------|
| $\text{Rh}(\text{PPh}_3)_2\text{H}_2\text{bpt}$                               |                                        | 0.96                                      |                           |
| $\text{Rh}(\text{PPh}_3)_2\text{H}_2\text{Hbpt}^+$                            |                                        | 1.13                                      |                           |
| $\text{Ru}(\text{bpy})_2\text{bpt}^+$                                         | 0.87 <sup>b</sup>                      |                                           | -1.47 (130)               |
|                                                                               |                                        |                                           | -1.73 (140)               |
| $(\text{bpy})_2\text{Ru}(\text{bpt})\text{RhH}_2-$<br>$(\text{PPh}_3)_2^{2+}$ | $E_{\text{a}} = 1.39$                  | 1.15                                      | -1.42 (80)                |
|                                                                               |                                        |                                           | -1.67 (90)                |
| $(\text{bpy})_2\text{Ru}(\text{bpt})\text{IrH}_2-$<br>$(\text{PPh}_3)_2^{2+}$ | $E_{\text{a}} = 1.24$                  | 1.12 <sup>c</sup>                         | -1.40 (65)                |
|                                                                               |                                        |                                           | -1.63 (75)                |
| $[\text{Ru}(\text{bpy})_2]_2\text{bpt}^{3+}$                                  | 1.08 <sup>a</sup><br>1.40 <sup>b</sup> | -1.39                                     | <sup>d</sup>              |

<sup>a</sup> In volts vs. SCE in  $\text{CH}_3\text{CN}/\text{TBAH}$  with scan rate = 100 mV/s<sup>b</sup> Reference 3<sup>c</sup> These values are approximate due to overlap of waves<sup>d</sup> Onset of complex electrochemistry at -1.39V (see text for details)

ruthenium bimetallic complex is probably a result of overlapping bpy-based redox couples.

The cyclic voltammograms of the protonated and deprotonated monometallic rhodium complexes,  $[\text{Rh H}_2(\text{PPh}_3)_2(\text{H}_n\text{bpt})](\text{PF}_6)_n$  ( $n = 0, 1$ ), exhibit only a single irreversible anodic wave while there is no observable reductive electrochemistry associated with either complex. The peak potential of the irreversible rhodium oxidation in the protonated monometallic complex is at 1.13V while in the deprotonated complex, it is at 0.96V.

The cyclic voltammograms of the heteronuclear bimetallic complexes  $[(\text{bpy})_2\text{Ru}(\text{bpt})\text{MH}_2(\text{PPh}_3)_2](\text{PF}_6)_2$  ( $M = \text{Ir}$  and  $\text{Rh}$ ), exhibit two overlapping oxidations and two well-behaved, one-electron reductions. The voltammogram of the iridium complex exhibits an irreversible anodic wave at -1.12V and an overlapping redox couple with  $E_{\text{a}} = 1.24$  and  $E_{\text{c}} = -1.14\text{V}$ . Due to severe overlap of the two redox processes these peak anodic potentials are only approximate. The two anodic waves at 1.15V and 1.39V in the rhodium bimetallic complexes are better defined than

those observed in the iridium complex. However, as in the iridium complex, overlap of the two redox processes precludes any accurate determination of the peak potential of the cathodic wave associated with the most positive anodic wave.

Due to the irreversible nature of the least positive redox process observed in the heteronuclear bimetallic complexes, this process is assigned as an irreversible iridium or rhodium oxidation.<sup>(1,13,14)</sup> The similarity between the anodic wave observed in the monometallic complex,  $[\text{RhH}_2(\text{PPh}_3)_2\text{bpt}]$ , and the least positive redox process observed in the rhodium heteronuclear bimetallic complex,  $[(\text{bpy})_2\text{Ru}(\text{bpt})\text{RhH}_2(\text{PPh}_3)_2](\text{PF}_6)_2$ , further support the above assignment. The presence of a cathodic wave associated with the most positive anodic wave suggests that this is a ruthenium based redox couple, i.e.,  $\text{Ru}^{\text{III/II}}$ .

The quantum yields obtained for the photoproduction of hydrogen from the bpt<sup>-</sup> complexes,  $\Phi_{\text{H}_2}$ , are given in Table III. The values obtained for

TABLE III.

Quantum Yields for the Photoproduction of  $\text{H}_2$  $\Phi_{\text{H}_2}$  (mols/ein)<sup>a</sup>

|                                                                          | $\lambda_{\text{ex}} = 365$  | $\lambda_{\text{ex}} = 313$  |
|--------------------------------------------------------------------------|------------------------------|------------------------------|
| $[\text{RhH}_2(\text{PPh}_3)_2\text{bpt}]$                               | $2.7 \pm 0.4 \times 10^{-2}$ | $1.3 \pm 0.2 \times 10^{-1}$ |
| $[(\text{bpy})_2\text{Ru}(\text{bpt})\text{RhH}_2(\text{PPh}_3)_2]^{2+}$ | $< 10^{-4}$                  | $2.6 \pm 0.6 \times 10^{-2}$ |
| $[\text{RhH}_2(\text{PPh}_3)_2\text{dpp}]^+$                             | $3.4 \pm 1.2 \times 10^{-2}$ | $1.3 \pm 0.2 \times 10^{-1}$ |

<sup>a</sup> In ethanol at 25°C.

the monometallic compounds,  $[\text{RhH}_2(\text{PPh}_3)_2(\text{H}_n\text{bpt})](\text{PF}_6)_n$  ( $n = 0$  and  $1$ ), are similar for both irradiation wavelengths used. The rhodium heteronuclear bimetallic complex,  $[(\text{bpy})_2\text{Ru}(\text{bpt})\text{RhH}_2(\text{PPh}_3)_2](\text{PF}_6)_2$ , exhibits very little photochemical production of molecular hydrogen ( $\Phi_{\text{H}_2} < 10^{-4}$ ) with an excitation wavelength of 365 nm. With an excitation wavelength of 313 nm,  $\Phi_{\text{H}_2} = 2.6 \times 10^{-2}$  which is about 25% of the quantum yield obtained in the monometallic complexes. The iridium heteronuclear bimetallic complex  $[(\text{bpy})_2\text{Ru}(\text{bpt})\text{IrH}_2(\text{PPh}_3)_2](\text{PF}_6)_2$  exhibits no photochemical production of hydrogen with  $\lambda_{\text{ex}} \geq 313\text{nm}$ .

## DISCUSSION

The absorption spectra of the rhodium monometallic complexes  $[\text{RhH}_2(\text{PPh}_3)_2(\text{H}_n\text{bpt})](\text{PF}_6)_n$  ( $n = 0$  and  $1$ ) exhibit a single high energy

maximum in the ultraviolet region which is assigned as the result of a  $\pi \rightarrow \pi^*$  transition. This assignment is primarily based on the similarity of the free ligand absorption spectrum and that of the monometallic complex. That the observed band is not MLCT in nature is supported by the absence of any ligand based reduction in the cyclic voltammograms. However, the lack of any ligand based reductions does not entirely exclude the possible existence of an MLCT transition as it has been shown that redox orbitals and optical orbitals may not directly correlate.<sup>(15)</sup> The trend in energies observed in both the free ligand and the monometallic complexes for these  $\pi \rightarrow \pi^*$  transitions (i.e.,  $E_{\text{protonated}} > E_{\text{deprotonated}}$ ) is readily attributed to the better  $\pi$  delocalization in the deprotonated ligand.

In previous studies of the photochemistry and photophysics of  $\text{RhH}_2(\text{PPh}_3)_2\text{L}^+$  (L = bpm, dpp, dpq, bpy, and ethylenediamine (en)),<sup>(1)</sup> the photochemistry and photophysics in acetone led to some interesting conclusions. The photophysics of these systems displayed an emission for L = bpm, dpp and bpy with the maximum of the excitation spectrum corresponding to a  $\text{Rh(III)} \rightarrow \text{L}$  MLCT generated emission. The photochemistry (i.e., loss of  $\text{H}_2$ ) was apparent for all complexes and had a wavelength dependence more consistent with involvement of an LF state. These interpretations suggest that the  $[\text{RhH}_2(\text{PPh}_3)_2(\text{H}_n\text{bpt})](\text{PF}_6)_n$  (n = 0 and 1) will show a wavelength dependence in the emission and photochemistry that is similar to bpm, dpp and dpq for n = 1, while requiring higher energy excitation wavelengths for n = 0 (reflecting the increase in LF energy expected for the inclusion of the anionic bpt<sup>-</sup> ligand). While both compounds show photoactivity at 365nm and little photochemistry at 405nm, the slightly larger reactivity for n = 1 at 405nm is in agreement with this assignment.

In previous studies of homonuclear and heteronuclear bimetallic complexes of the type  $([\text{Ru}(\text{bpy})_2]_2\text{L})(\text{PF}_6)_4$ <sup>(7-12)</sup> and  $(\text{bpy})_2\text{RuLMH}_2(\text{PPh}_3)_2(\text{PF}_6)_3$  (M = Ir and Rh; L = bpm, dpp and dpq),<sup>(1)</sup> it was shown that the MLCT transition absorption maxima shifts to lower energy relative to the absorption maxima observed in the ruthenium monometallic complex,  $[\text{Ru}(\text{bpy})_2\text{L}](\text{PF}_6)_2$ . Also, the reduction potentials associated with the  $\text{L}^0/\text{L}^+$  redox couple in these previously studied homonuclear and heteronuclear bimetallic complexes shift to more positive potentials relative to the ruthenium monometallic complex. This behavior has been interpreted to result from substantial stabilization of the  $\pi^*$  orbitals associated with the bridging ligand. The fact that the lowest energy  $\pi^*$  orbital is associated with the bridging ligand in the bimetallic and the monometallic is supported by emission<sup>(9-12)</sup> and resonance Raman<sup>(9)</sup> studies.

In the complexes with  $\text{bpt}^-$  as a bridging ligand the behavior described above is not observed. In both the heteronuclear bimetallic complexes studied,  $[(\text{bpy})_2\text{Ru}(\text{bpt})\text{MH}_2(\text{PPh}_3)_2](\text{PF}_6)_2$  ( $\text{M} = \text{Ir}$  and  $\text{Rh}$ ), and the reported homonuclear complex,  $[(\text{Ru}(\text{bpy})_2)_2\text{bpt}](\text{PF}_6)_3$ , the absorption and emission maxima shift to higher energy relative to the observed spectrum of the monometallic complex,  $[\text{Ru}(\text{bpy})_2\text{bpt}](\text{PF}_6)$ . The reduction potentials of the bimetallic complexes do shift slightly positive relative to the monometallic complex; however, this is probably a coulombic effect due to the increased charge on the bimetallic complexes. This behavior and the fact that only two bpy related reductions are observed in the complexes,  $[\text{Ru}(\text{bpy})_2\text{bpt}]\text{PF}_6$  and  $[(\text{bpy})_2\text{Ru}(\text{bpt})\text{MH}_2(\text{PPh}_3)_2](\text{PF}_6)_2$  ( $\text{M} = \text{Ir}$  and  $\text{Rh}$ ), implies that the lowest energy MLCT transitions in all  $\text{bpt}^-$  complexes are  $\text{Ru} \rightarrow \text{bpy}$  MLCT in nature. This assignment is supported by the recently published resonance Raman study on the complexes  $[\text{Ru}(\text{bpy})_2\text{bpt}]\text{PF}_6$  and  $[(\text{Ru}(\text{bpy})_2)_2\text{bpt}](\text{PF}_6)_3$ .<sup>(4)</sup> In this study, excitation at wavelengths of 458, 488, and 514.5nm showed only enhancement of bpy vibrations.

The room temperature emission observed in the heteronuclear complexes  $[(\text{bpy})_2\text{Ru}(\text{bpt})\text{MH}_2(\text{PPh}_3)_2]^{3+}$  ( $\text{M} = \text{Ir}$  and  $\text{Rh}$ ) are assigned as the result of a  $\text{Ru} \rightarrow \text{bpy}$  MLCT transition. This assignment is based on the energy of the emission and excitation maxima and the resonance Raman study mentioned previously.<sup>(4)</sup>

The interesting feature of the emission data is the quantum yields. In complexes in which the  $\pi^*$  energy level of the bridging ligand is less than that of the bpy ligand, i.e.,  $\text{L} = \text{dpp}$ ,  $\text{dpq}$  and  $\text{bpm}$ , quantum yields decrease when comparing the monometallic to bimetallic complexes. This is the case for both the homonuclear<sup>(9-12)</sup>,  $[(\text{bpy})_2\text{Ru}_2\text{L}]^{4+}$  and heteronuclear<sup>(1)</sup>,  $[(\text{bpy})_2\text{RuLRhH}_2(\text{PPh}_3)_2]^{3+}$ , bimetallic complexes. In the case of  $\text{bpt}^-$  as the bridging ligand, where now the  $\pi^*$  energy of the bridging ligand orbital is higher than the bpy ligand, the quantum yield for emission decreases for the homonuclear bimetallic complex  $[(\text{bpy})_2\text{Ru}_2\text{bpt}]^{3+}$  but increases for the heteronuclear bimetallic complexes  $[(\text{bpy})_2\text{Ru}(\text{bpt})\text{MH}_2(\text{PPh}_3)_2]^{2+}$  ( $\text{M} = \text{Ir}$  and  $\text{Rh}$ ) when compared to the monometallic complex  $[\text{Ru}(\text{bpy})_2\text{bpt}]^+$ .

An explanation for this anomalous behavior comes from looking at the effect of the perturbation of a second metal center on the emitting chromophore, a  $\text{Ru} \rightarrow \text{bpy}$  MLCT excited state. When the rhodium metal center is added to the  $\text{bpt}^-$  ligand, the  $\text{bpt}^- \pi^*$  system is lowered in energy and competes more favorably with bpy for  $\pi$ -backbonding from the  $\text{Ru}(\text{II})$  center. Thus, even though the bpy  $\pi^*$  level is still lower than the  $\text{bpt}^- \pi^*$  level, the difference is smaller and the  $\text{Ru} \rightarrow \text{bpy}$  MLCT absorption and emission bands are at higher energy for the heterobimetallic complex. The

larger energy gap gives rise to a longer excited-state lifetime and a higher emission quantum yield. The same arguments can be used for the position of the absorption and emission maxima of the homobimetallic complex,  $\{[(bpy)_2Ru]_2bpt\}^{3+}$ . However, the quantum yield for emission in this case is lower than the monometallic analog due to the similarity in the two metal centers involved in the deactivation of the excited state.

The photophysical properties of  $(bpy)_2Ru(bpt)RhH_2(PPh_3)_2^{2+}$  are different than complexes bridged by bpm, dpp and dpq mainly due to the  $Ru \rightarrow bpy$  MLCT-based emission of the former and the  $Ru \rightarrow L$  MLCT-based emission of the latter. The photochemical differences are harder to rationalize. In the previous studies (in acetone) for  $L = bpm, dpp$  and  $dpq$ , photoinduced reductive elimination of  $H_2$  occurs at  $\lambda_{ex} \leq 436$  nm. This corresponds to irradiation above the lowest spectroscopically available state and is thought to result from population of a  $Ru \rightarrow bpy$  MLCT state, a  $Ru/Rh \rightarrow L$  MLCT state involving a higher  $\pi^*$  level on L, or a combination of the two. For the  $L = bpt^-$  case described here, the bridging ligand  $\pi^*$  orbitals are pushed up in energy as is the threshold energy for photochemistry.

The higher threshold energy needed for  $H_2$  production from  $(bpy)_2Ru(bpt)RhH_2(PPh_3)_2^{2+}$  could result from a number of occurrences. First of all, it could reflect an increase in energy in the rhodium-based photoactive state in going from neutral diimine or diamine ligand to  $bpt^-$ . This doesn't appear to be significant since there is only a small difference in the photochemical behavior of  $RhH_2(PPh_3)_2bpt$  and  $RhH_2(PPh_3)_2dpp^+$  (Table III). A more likely explanation is that energy transfer from the absorbing state (probably localized mainly on Ru) to the reactive state on Rh requires orbital participation of the bridging ligand. Because the  $bpt^- \pi^*$  orbitals are so elevated in energy vs. those of bpm, dpp and dpq in  $(bpy)_2RuLRhH_2(PPh_3)_2^{n+}$ , the threshold photochemical energy is much higher for the former.

An interesting comparison of two luminative complexes appears in Table IV. All values in Table IV for  $(bpy)_2Ru(dpp)RhH_2(PPh_3)_2^{3+}$  and  $(bpy)_2Ru(bpt)RhH_2(PPh_3)_2^{2+}$  are reported in ethanol as a solvent. The difference in absorption, emission, and excitation maxima in the two complexes is the result of  $Ru \rightarrow dpp$  MLCT involvement in the former and  $Ru \rightarrow bpy$  MLCT involvement in the latter. The more interesting data deals with the wavelength dependence of the photochemical and emission quantum yields.

TABLE IV.  
Comparison of dpp and bpt<sup>-</sup> Complexes<sup>a</sup>

| Properties             | (bpy) <sub>2</sub> RudppRh(PPh <sub>3</sub> ) <sub>2</sub> H <sub>2</sub> <sup>3+</sup> | (bpy) <sub>2</sub> RubptRh(PPh <sub>3</sub> ) <sub>2</sub> H <sub>2</sub> <sup>2+</sup> |                        |                             |
|------------------------|-----------------------------------------------------------------------------------------|-----------------------------------------------------------------------------------------|------------------------|-----------------------------|
| λ <sub>max</sub> (abs) | 488 nm                                                                                  | 459 nm                                                                                  |                        |                             |
| λ <sub>max</sub> (em)  | 757 nm                                                                                  | 630 nm                                                                                  |                        |                             |
| λ <sub>max</sub> (ex)  | 476 nm                                                                                  | 468 nm                                                                                  |                        |                             |
| λ <sub>irr</sub>       | Φ <sub>H2</sub>                                                                         | Φ <sub>em</sub>                                                                         | Φ <sub>H2</sub>        | Φ <sub>em</sub>             |
| 436 nm                 | <10 <sup>-4</sup>                                                                       | 3.0 ± 2 x 10 <sup>-2</sup>                                                              | ----                   | 1.3 ± .1 x 10 <sup>-2</sup> |
| 405 nm                 | 4.4 ± 0.6 x 10 <sup>-3</sup>                                                            | 2.8 ± .2 x 10 <sup>-3</sup>                                                             | ----                   | 1.2 ± .1 x 10 <sup>-2</sup> |
| 365 nm                 | 4.6 ± 0.4 x 10 <sup>-3</sup>                                                            | 3.0 ± .2 x 10 <sup>-3</sup>                                                             | <10 <sup>-4</sup>      | 1.1 ± .1 x 10 <sup>-2</sup> |
| 313 nm                 | 5.6 ± 0.8 x 10 <sup>-2</sup>                                                            | 5.0 ± 8 x 10 <sup>-3</sup> b                                                            | 2.6 x 10 <sup>-2</sup> | 3.7 ± .2 x 10 <sup>-3</sup> |

<sup>a</sup> In ethanol at 25°C.

<sup>b</sup> Upper limit, some emissive photoproducts generated.

The interpretation of the bpt<sup>-</sup> bridged complex, (bpy)<sub>2</sub>Ru(bpt)RhH<sub>2</sub>-(PPh<sub>3</sub>)<sub>2</sub><sup>2+</sup> is straight forward. The emission quantum yield is invariable at longer wavelengths where no photochemistry occurs. With the onset of photochemistry at 313 nm, the emission quantum yield decreases as the energy is partitioned into the photochemically reactive state. Assuming that the emission quantum yield would be constant if photochemistry did not occur, we can calculate a partitioning at 313 nm of 70% into the photochemical channel and 30% into the emission channel. The interrelationship of ruthenium-based emission and rhodium-based photochemistry in the bpt<sup>-</sup> bridged system is the strongest evidence to date for intramolecular energy transfer in these systems.

The wavelength dependence for the dpp bridged system, (bpy)<sub>2</sub>Ru(bpt)RhH<sub>2</sub>(PPh<sub>3</sub>)<sub>2</sub><sup>2+</sup>, is more difficult to explain. From Table IV, the emission quantum yield is virtually unchanged over the range of irradiation wavelengths. However, the photochemical quantum yield shows a dramatic wavelength sensitivity which implies that there is an initial energy partitioning that explains the wavelength-independent emission yield and a secondary partitioning of the remaining excited states to give wavelength-dependent photochemistry. Since quantum yields for both photochemistry and photophysics are calculated from total absorbance of the molecule, this behavior is not due to the two metal centers acting as separate, uncoupled entities. However, the complexity of the photochemistry and the simplicity of the photophysics indicate that the interconversions occurring in this system must involve a minimum of

three excited states of which one is a ruthenium-based emissive state and another is a rhodium-based reactive state.

#### ACKNOWLEDGMENT

The authors acknowledge the U.S. Department of Energy (DE-FG 09-87ER13768) for support of this work.

#### REFERENCES

- 1 D. B. MacQueen and J. D. Petersen, submitted for publication.
- 2 R. J. Watts, J. S. Harrington and J. Van Houten in: M. S. Wrighton (ed), Inorganic and Organometallic Photochemistry: Advances in Chemistry Series #168, American Chemical Society, Washington, D. C., 1978, pp 57-72.
- 3 R. Hage, A. H. J. Dijkhuis, J. G. Haasnoot, R. Prins, J. Reedijk, B. E. Buchanan, and J. G. Vos, *Inorg. Chem.*, **27**(12) (1988) 2185.
- 4 R. Hage, J. G. Haasnoot, D. J. Stufkins, T. L. Snoeck, J. G. Vos and J. Reedijk, *Inorg. Chem.*, **28**(7) (1989) 1413.
- 5 J. F. Geldard and F. Lions, *J. Org. Chem.*, **30** (1965) 318.
- 6 J. A. Osborn and R. R. Schrock, *J. Am. Chem. Soc.*, **93** (1971) 2397.
- 7 M. Hunziker and A. Ludi, *J. Am. Chem. Soc.*, **99** (1977) 7370.
- 8 D. P. Rillema and K. B. Mack, *Inorg. Chem.*, **21**(10) (1982) 3849.
- 9 C. H. Braunstein, A. D. Baker, T. C. Streckas, and H. D. Gaffney, *Inorg. Chem.*, **23**(7) (1984) 857.
- 10 A. Juris, V. Balzani, F. Barigelli, P. Belser and A. Von Zelewsky, *Coord. Chem. Revs.* **84** (1988) 85-277.
- 11 J. D. Petersen, in: V. Balzani (ed) Supramolecular Photochemistry: NATO ASI Series C, Vol. 214, D. Reidel, Dordrecht, Holland, 1987, pp 135-152.
- 12 E. V. Dose and L. J. Wilson, *Inorg. Chem.*, **17**(9) (1978) 2660.
- 13 G. Kew, M. K. DeArmond and K. W. Hanck, *J. Phys. Chem.*, **78**(7) (1974) 727.
- 14 J. L. Kahl, K. W. Hanck and M. K. DeArmond, *J. Phys. Chem.*, **82**(5) (1978) 540.
- 15 Y. Ohsawa, K. W. Hanck and M. K. DeArmond, *J. Electroanal. Chem.*, **175** (1984) 229.